



New insights into chlorantraniliprole metabolic resistance mechanisms mediated by the striped rice borer cytochrome P450 monooxygenases: A case study of metabolic differences



Lu Xu ^{a,*}, Jun Zhao ^b, Dejin Xu ^a, Guangchun Xu ^a, Yingchuan Peng ^{c,*}, Yanan Zhang ^d

^a Key Lab of Food Quality and Safety of Jiangsu Province-State Key Laboratory Breeding Base, Institute of Plant Protection, Jiangsu Academy of Agricultural Sciences, Nanjing 210014, China

^b Key Laboratory of Green Preservation and Control of Tobacco Diseases and Pests in the Huanghuai Growing Area, Institute of Tobacco Research, Henan Academy of Agricultural Sciences, Xuchang 461000, China

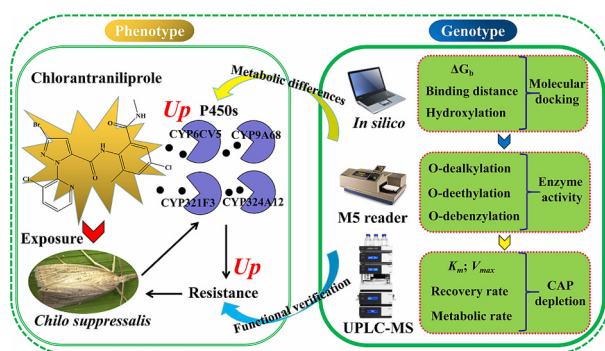
^c Institute of Entomology, Jiangxi Agricultural University, Nanchang 330045, China

^d Anhui Engineering Research Center for Green Production Technology of Drought Grain Crops, College of Life Sciences, Huaipei Normal University, Huaipei 235000, China

HIGHLIGHTS

- The metabolic mechanisms of CAP resistance were revealed at the protein level.
- The resistance to CAP had increased its use, increasing environmental pollution.
- The recombinant P450s showed significant metabolism differences to CAP.
- The P450s mediated CAP metabolic resistance through joint action in SSB.
- Unraveling the link between over-expression levels and catalytic activities of P450s.

GRAPHICAL ABSTRACT



ARTICLE INFO

Editor: Daqiang Yin

Keywords:
Chilo suppressalis
Insecticide resistance
Genome alignment

ABSTRACT

The anthranilic diamide insecticide chlorantraniliprole has been extensively applied to control Lepidoptera pests. However, its overuse leads to the development of resistance and accumulation of residue in the environment. Four P450s (*CYP6CV5*, *CYP9A68*, *CYP321F3*, and *CYP324A12*) were first found to be constitutively overexpressed in an SSB CAP-resistant strain. It is imperative to further elucidate the molecular mechanisms underlying P450s-mediated CAP resistance for mitigating its environmental contamination. Here, we heterologously expressed these four P450s in insect cells and evaluated their abilities to metabolize CAP. Western blotting and

Abbreviations: P450, cytochrome P450 monooxygenase; CAP, chlorantraniliprole; SSB, striped rice borer; CO, carbon monoxide; EST, esterase; GST, glutathione-S-transferase; UGT, uridine diphosphate-glycosyl transferase; NADPH, nicotinamide adenine dinucleotide phosphate; CuOOH, cumene hydroperoxide; CPR, cytochrome P450 reductase; RyR, ryanodine receptors; MOI, multiplicity of infection; TBST, tris-buffered saline containing Tween 20; EC, 7-ethoxycoumarin; MR, 7-methoxyresorufin; EFC, 7-ethoxy-4-trifluoromethyl coumarin; BFC, 7-benzyloxy-4-trifluoromethyl coumarin; UPLC-MS, ultra performance liquid chromatography-mass spectrometry; MRM, multiple reaction monitoring; PCR, polymerase chain reaction.

* Corresponding authors.

E-mail addresses: xulupesticide@163.com (L. Xu), ycpeng@jxau.edu.cn (Y. Peng).

<https://doi.org/10.1016/j.scitotenv.2023.169229>

Received 8 October 2023; Received in revised form 30 November 2023; Accepted 7 December 2023

Available online 8 December 2023

0048-9697/© 2023 The Authors. Published by Elsevier B.V. This is an open access article under the CC BY-NC-ND license (<http://creativecommons.org/licenses/by-nc-nd/4.0/>).

Heterologous expression
Probe substrates
Computational simulation

reduced CO difference spectrum tests showed that these four P450 proteins had been successfully expressed in S9 cells, which are indicative of active functional enzymes. The recombinant proteins CYP6CV5, CYP9A68, CYP321F3, and CYP324A12 exhibited a preference for metabolizing the fluorescent P450 model probe substrates EC, BFC, EFC, and EC with enzyme activities of 0.54, 0.67, 0.57, and 0.46 pmol/min/pmol P450, respectively. *In vitro* metabolism revealed distinct CAP metabolic rates (0.97, 0.86, 0.75, and 0.55 pmol/min/pmol P450) and efficiencies (0.45, 0.37, 0.30, and 0.17) of the four recombinant P450 enzymes, thereby elucidating different protein catalytic activities. Furthermore, molecular model docking confirmed metabolic differences and efficiencies of these P450s and unveiled the hydroxylation reaction in generating *N*-demethylation and methylphenyl hydroxylation during CAP metabolism. Our findings not only first provide new insights into the mechanisms of P450s-mediated metabolic resistance to CAP at the protein level in SSB but also demonstrate significant differences in the capacities of multiple P450s for insecticide degradation and facilitate the evaluation and mitigation of toxic risks associated with CAP application in the environment.

1. Introduction

Insecticide resistance continuously threatens pest control, and over 600 insect and mite species have developed resistance to insecticides (Sparks et al., 2020). However, chemical insecticides are still used as a major strategy for controlling pests, and their overuse in repeated spraying further exacerbates the development of resistance (Bass and Nauen, 2023). As a result, there has been a global trend to reduce environmental risks caused by insecticides via insecticide resistance management. Understanding the mechanisms of insecticide resistance is a vital first step for resistance management (Ju et al., 2021). During the initial stage of insecticide application, insects are prone to exposure to low concentrations because insecticide concentrations usually vary in the environment due to migration, leaching, degradation, unreasonable use, and behavioral avoidance (Margus et al., 2024). Insects can rapidly evolve metabolic resistance to insecticides at low concentrations via enhanced detoxification enzymes, such as P450, EST, GST, and UGT. Metabolic resistance is a biochemical transformation process of xenobiotics that prevents insecticides from reaching insect molecular targets and increases the excretion of insecticides (Li et al., 2024). Therefore, it is important to unveil the metabolic resistance mechanisms of insecticides.

A large number of studies have shown that P450s have been implicated in insecticide resistance in insects (Nauen et al., 2022). The insect P450 is the most important detoxification enzyme superfamily of hem-e-thiolate proteins and can catalyze insecticides into less-toxic metabolites during phase I metabolism. The P450-based insecticide metabolic resistance is typically mediated by hydroxylation, dealkylation and other oxidative reactions, which is often involved in the increased expression of one or more P450 genes (Lu et al., 2021). CAP resistance in lab-selected and field strains of *Plutella xylostella* and *Spodoptera exigua* is related to the CYP6, CYP9, and CYP321 families of the CYP3 clan that often participate in insecticide detoxification and metabolic resistance (Hu et al., 2014; Li et al., 2018; Wang et al., 2018). Although several P450s associated with the resistance trait have been identified, the exact role of P450s and their actual contribution to the resistance phenotype remain largely unknown. The enhanced metabolic detoxification of insecticides in insects is closely associated with an increase in P450 protein production and enzymatic activity (Lu et al., 2021). Functional *in vitro* characterization approaches can be employed to validate the differential expressions and activities of P450 proteins associated with an insecticide-resistance phenotype.

Chlorantraniliprole, the first anthranilic diamide insecticide according to the Insecticide Resistance Action Committee mode of action classification, is recommended for controlling lepidopteran pest species (Xu et al., 2022; Yin et al., 2023), and its registration scope ranges from agricultural crops to ornamentals and turf grass in residential and public areas (Rodrigues et al., 2015). The global market value of CAP had reached USD 1886.8 million in 2022. It binds to RyR that are large homotetrameric calcium-release channels located in the *endo*- and sarcoplasmic reticulum, and triggers the uncontrolled release of the calcium stores, causing feeding cessation, paralysis, and death of insects

(Haas et al., 2022). While mammals possess three RyR isoforms, insects only encode one RyR gene. Therefore, CAP exhibits high activity against pests and low toxicity to mammals due to the RyR structural differences between insects and mammals (Ferreira et al., 2022). However, its frequent use has led to intensified resistance selection pressure on agricultural pests over the past 10 years, and amino acid substitutions in the transmembrane domain of the RyR associated with reduced CAP efficacy have been identified in *P. xylostella*, *Spodoptera frugiperda*, and *Chilo suppressalis* (Richardson et al., 2020). Subsequently, the current resistance levels of CAP have caused its overuse in lepidopteran pest management, enhancing the risk of CAP to the environment. According to reports, the application of chemical insecticides has led to the death of non-target insects and pollution of air, water, and soil as well as threats to human health (Ibrahim et al., 2020a; Ibrahim et al., 2022; Lu et al., 2023; Yang et al., 2021).

The striped rice borer, *C. suppressalis* (Walker) (Lepidoptera: Crambidae), is a devastating rice pest that is prevalent in Asia, the Middle East, and southern Europe. It damages rice crops by boring into and feeding on their stems, increasing rice yield losses (Su et al., 2014; Yang et al., 2021). Currently, the control of SSB mainly depends on the use of chemical insecticides. CAP has excellent bottom-up intake and transportation in plants and effectively penetrates plants from root to stem (Wang et al., 2021). The CAP has been widely used to control SSB in paddy fields; however, it has developed high resistance to CAP over the past decade (Huang et al., 2021). Although RyR target-site mutations contribute to a high level of CAP resistance in SSB, P450s play a role in the detoxification of CAP. A previous study had shown that the overexpression of four P450 genes (CYP6CV5, CYP9A68, CYP321F3, and CYP324A12) was found in an SSB CAP-selected strain. These four P450s from the CYP3 clan might be new potential candidates for conferring CAP resistance (Xu et al., 2019). However, the absence of a link between the overexpression levels and actual catalytic activities of these four P450s nullifies such a conclusion regarding P450s-mediated CAP metabolic resistance. Some studies have functionally characterized the catalytic activities of P450s with heterologous expression to insecticides *in vitro*, e.g., CYP6P3, CYP6M2, CYP6Z1, and CYP9K1 from *Anopheles gambiae* and CYP9M6, CYP6BB2, CYP9J24, CYP9J26, CYP6J28, and CYP9J32 in *Aedes aegypti*, which confirmed that upregulated P450s confer insecticide resistance (Vontas et al., 2020). Moreover, whether the roles of P450 genes are through joint or single actions in CAP metabolic resistance remains unclear.

The aim of this study was to determine whether four overexpressed P450s in CAP-resistant strains of SSB had the potential to produce recombinant enzymes capable of metabolizing CAP. Moreover, computational molecular modeling simulation was performed to reveal the docking of the four P450 models with CAP. These findings will elucidate the roles of multiple P450s in CAP resistance and their metabolic differences at the protein level.

2. Materials and methods

2.1. Insecticides and chemicals

The CAP standard (CAS Number 500008-45-7) was purchased from the Laboratory of the Government Chemists (London, England). Pri-meSTAR HS DNA polymerase, restriction endonuclease, and T4 ligase were supplied by Takara Bio Inc. (Dalian, China). The model substrates and NADPH and CuOOH were obtained from Sigma-Aldrich (St Louis, MI, USA). The NADPH regeneration system was purchased from Promega Corp. (Madison, WI, USA). The Bac-to-Bac baculovirus expression system and chromatographic solvents were purchased from Thermo Fisher Scientific (Waltham, MA, USA). The pFastBac1 vector and the *Escherichia coli* DH10Bac competent cells were obtained from our laboratory.

2.2. P450 gene identification and sequence analysis

CYP6CV5 (GenBank accession number MH001161.1), *CYP9A68* (GenBank accession number MH001162.1), *CYP321F3* (GenBank accession number MH001163.1), and *CYP324A12* (GenBank accession number MH001164.1) were obtained from the WHR strain as described by Xu et al. (2019). The transcript sequences of these four P450 genes were aligned to the SSB genome (https://www.ncbi.nlm.nih.gov/assembly/GCA_902850365.2). The exons, introns, corresponding chromosomes, and specific base positions of the four P450 genes located on the genome sequence were analyzed.

2.3. Homology modeling and substrate docking

The homology model of P450 was constructed by submitting the sequence to the I-TASSER server for automated protein structure prediction (Roy et al., 2010). A molecular model of P450 with CAP was created using the molecular modeling software SYBYLx2.0 (Certara, St Louis, MO, USA). Visualization and display of the amino acid residues and electrostatic surface potential on the homologous structure were conducted using the PyMOL Molecular Graphics System v.1.5.0.4 (Schrödinger, New York, NY, USA). The resulting raw model was subjected to energy minimization using SYBYLx2.0 to remove distortions and unallowed van der Waals' contacts resulting from the molecular modeling process. The details have been displayed in the Supplementary Material.

2.4. Heterologous expression in *Sf9* cells

An insect baculovirus expression system was used to express recombinant P450 proteins (Elzaki et al., 2017; Shi et al., 2022; Wang et al., 2017). P450s and CPR primers were designed with restriction sites before the Kozak sequences at the start codon and before the stop codon for the sense and the anti-sense primers, respectively (Table S1). Both P450 and CPR were fused to the pFastBac1 vector and transformed into DH10Bac competent cells for baculovirus construction. Non-insertion pFastBac1 was used as a negative control. Recombinant bacmid DNAs were extracted according to the manufacturer's instructions and transfected into *Sf9* cells. The viral titer was determined using the recommended protocol. When the cell density reached 2×10^6 cells/mL, they were co-infected with recombinant baculoviruses with P450s (or non-insertion controls) and CPR at an MOI ratio of 2 and 0.2, respectively. The cells were collected after 48 h of culture and washed thrice with phosphate-buffered saline (Yuanye, Shanghai, China). Microsomes were prepared using differential centrifugation according to standard procedures and stored at -80°C . The total microsomal content was measured using the Bradford method (Shi et al., 2018).

The expression of recombinant P450s and CPR isolated from baculovirus-infected insect cells were assessed using a 6 \times His Tag antibody (Abcam, Cambridge, UK). Briefly, proteins were separated

using sodium dodecyl-sulfate polyacrylamide gel electrophoresis and then electrotransferred to a polyvinylidene difluoride membrane (Merck-Millipore, MA, USA) at 4°C and 40 V overnight. Subsequently, the membrane was washed thrice with TBST. The membrane was blocked with 5 % bovine serum albumin for 2 h at 30°C . After washing thrice with TBST, the membrane was incubated for 1 h at 25°C with a Tag mouse monoclonal antibody (Abcam, Cambridge, UK). Furthermore, the membrane was washed thrice with TBST and incubated with goat anti-mouse IgG antibodies (Abcam, Cambridge, UK) for 1 h at 25°C . After washing for 5 min with TBST, the membrane was incubated for 5 min with chromogen solution and enhancement solution (1:1) and checked for antibody-reactive bands using an imaging system (Bio-Rad, Hercules, CA, USA). Microsomes from uninfected *Sf9* insect cells were used as the controls.

All the expressed recombinant P450s were measured using reduced CO difference spectrum assay (Shi et al., 2018). The recombinant P450 was diluted to 1 mg/mL with 0.1 M potassium phosphate buffer (pH 7.4) containing 20 % glycerol, and approximately 1 mg of sodium dithionite was added as the reducing agent. After recording the absorption spectrum at 500–400 nm as a baseline, CO gas was introduced into the recombinant P450 mixture for 1 min at a speed of 1–2 bubbles, and the absorption spectrum (500–400 nm) change was measured. The recombinant P450 concentration was calculated using the Abs450-Abs490/0.091/protein concentration, and expressed as pmol P450/mg protein.

2.5. P450 enzyme activities on model substrates

Four traditional fluorescent P450 model probe substrates, including EC, MR, EFC, and BFC, were used to identify O-dealkylation, O-debenzylation, and O-deethylation reactions of recombinant P450s in microplates (Shi et al., 2018; Shi et al., 2022). All assays were performed in a total volume of 200 μL containing 0.1 M potassium phosphate buffer (pH 7.4) and 0.1 mg microsomes of P450/CPR. All substrates were dissolved with DMSO and DMSO $\leq 1\%$ in a $>200\text{ }\mu\text{L}$ reaction system. Microsomes and substrates were incubated with NADPH or CuOOH at 30°C for 5 min before initiating the reaction. Reactions were performed in black 96-well plates using a Spectra Max M5 reader (Molecular Devices, Silicon Valley, CA, USA). In the MROD test for P450 O-demethylation activity, microplates with 10 μM MR and 10 mM NADPH were read every 30 s at 530 nm/585 nm (excitation/emission wavelengths) for 30 min. In the ECOD and EFCOD reactions for P450 O-deethylation activity, microplates with 100 μM EC and 25 μM EFC by adding 10 mM NADPH and 500 mM CuOOH were monitored every 30 s at 370 nm/450 nm and 410 nm/538 nm (excitation/emission wavelengths) for 30 min, respectively. CuOOH was used as the electron source to eliminate the interference from NADPH fluorescence. The BFCOD reaction for P450 O-debenzylation activity with 25 μM BFC and 10 mM NADPH was monitored under the same conditions as those for EFCOD. Wells containing the microsome from uninfected *Sf9* cells served as controls. Each recombinant P450/substrate solution was tested in triplicate. Metabolic activity was expressed as pmol product/minute/pmol P450.

2.6. Analysis of CAP metabolism

Analysis of CAP metabolism using recombinant P450/CPR microsome was performed in 200 μL 0.1 M potassium phosphate buffer (pH 7.4), including 0.2 mg recombinant P450, NADPH regeneration system (1.3 mM NADP⁺, 3.3 mM glucose-6-phosphate, 3.3 mM MgCl₂, and 0.5 U/mL glucose-6-phosphate dehydrogenase), and 20 μM CAP. This reaction system was incubated in a metal bath at 30°C for 5 min before adding CAP and being put on a thermostatic oscillator to incubate at 30°C and 1200 rpm for 1 h. Reactions were stopped after adding 200 μL ice-cold acetonitrile. Then, 600 μL dilution buffer, including 50 % acetonitrile and 50 % potassium phosphate buffer, was added to each reaction mixture and incubated for a further 20 min at 30°C at 1200 rpm to ensure insecticide dissolution. The supernatant was collected from the

quenched reactions using centrifugation at 20,000g for 10 min and injected into chromatograph vials for UPLC-MS analysis immediately after filtering using a 0.22 µm filter. Negative controls with an equivalent weight of non-insertion microsomes and without the NADPH regeneration system were used (Shi et al., 2022). In the UPLC-MS analysis, the excimer ion and fragmentation rule of the substrate were verified using primary and secondary mass spectrometry. MRM was performed to quantify and qualify CAP. CAP was assessed using isocratic elution with acetonitrile and water/0.1 % (v/v) acetic acid as the mobile phase (5 min acetonitrile:H₂O 70:30) using Waters Acquity UPLC BEH C18 (particle diameter 1.7 µm, 100 mm × 2.1 mm), flowing at 0.3 mL/min and with a column temperature of 40 °C detected in the positive

electrospray ionization ion mode (Wu et al., 2018b). Substrate reduction was used as a criterion for assessing P450 enzyme activity. Substrate degradation was quantified using an external standard method. The injection volume for each sample was 5 µL. The final metabolic activity was corrected by subtracting the background (uninfected Sf9 cell control) and expressed as pmol CAP disappearance/min/pmol P450. For enzyme reaction kinetics of CAP metabolism, different ranges of CAP concentrations were used for different P450s. Recombinant P450 (20 pmol) and a suitable incubation time were selected for each P450. Samples were analyzed as described above. The kinetic parameters maximum velocity (V_{max}) and Michaelis constant (K_m) were determined using nonlinear regression analysis of GraphPad Prism 8.0.2 software

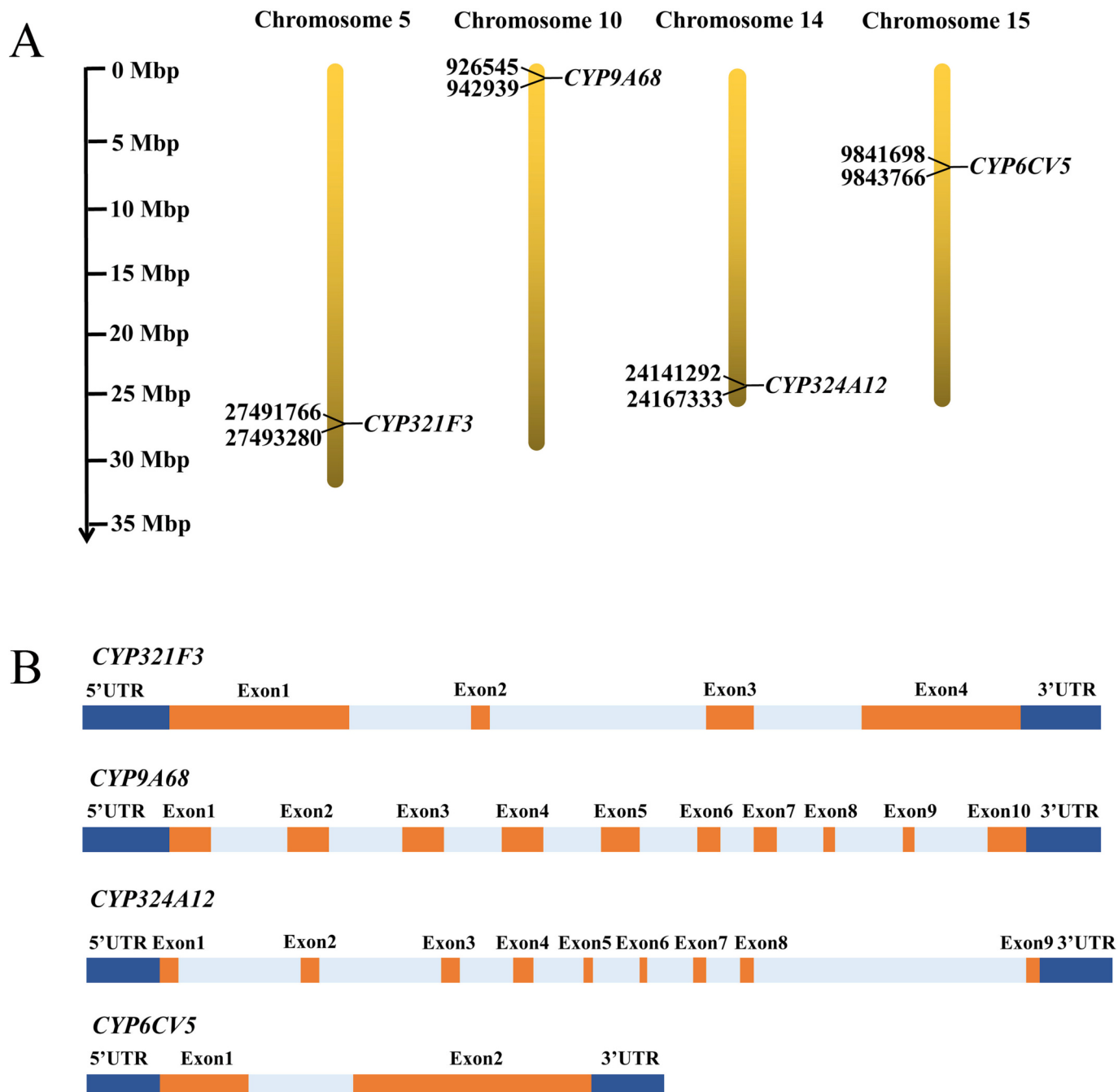


Fig. 1. Profiles of P450s *CYP6CV5*, *CYP324A12*, *CYP321F3*, and *CYP9A68* in the striped rice borer. A. The base positions of four P450 genes on the chromosome are marked on the left of the gold column which represents the chromosome. B. The deoxyribonucleic acid structures of four P450 genes. Orange and blue boxes represent exon and untranslated region.

(Franklin Street, Boston, MA, USA) (Shi et al., 2022). Each treatment was repeated thrice.

2.7. Statistical analysis

Data are expressed as the means \pm standard deviations (SD). One-way analysis of variance (ANOVA) followed by Tukey's honest significant difference (HSD) test was used for multiple group comparisons. All statistical analyses were performed using SPSS 25.0 software (SPSS Inc., Chicago, IL, USA). $P < 0.05$ was considered statistically significant.

3. Results

3.1. Confirmation of P450 gene sequence

To ensure the integrity and accuracy of the P450 transcript sequences, we performed genome alignment analysis. Fig. 1A showed that the base positions of CYP321F3, CYP9A68, CYP324A12, and CYP6CV5 on parallel chromosomes spanned between 27,491,766 and 27,493,280 bp, 926,545 and 942,939 bp, 24,141,292 and 24,167,333 bp, and 9,841,698 and 9,843,766 bp, respectively, which were located on chromosomes 5, 10, 14, and 15 in SSB, respectively. The number order of exons on the genome sequences of the P450 transcripts was CYP9A68 (10) > CYP324A12 (9) > CYP321F3 (4) > CYP6CV5 (2) (Fig. 1B). These results provided an essential sequence basis for subsequent heterologous expression of P450 genes.

3.2. P450 modeling and chlorantraniliprole docking

To rationalize the metabolic differences of recombinant P450s, *in silico* docking simulation with CAP at the active site of each P450 was performed. The protein models of CYP6CV5, CYP324A12, CYP321F3, and CYP9A68 were generated, and the estimated free energies (ΔG_b) of CAP bound with these P450 proteins were -7.5 , -7.1 , -7.3 , and -7.4 kcal/mol, respectively (Table 1), thus indicating that CYP6CV5 was the most tightly bound to CAP, followed by CYP9A68, CYP321F3, and CYP324A12. Simultaneously, we also analyzed the binding distance between CAP and the heme of the P450 proteins. The results demonstrated that the hemes of CYP6CV5 and CYP321F3 were contacted *N*-methyl carbons of the anthraniloyl moiety of CAP with distances of 2.9 and 4.3 Å, and the hemes of CYP324A12 and CYP9A68 were 5.1 and 4.0 Å from the docked methylphenyls of the anthraniloyl moiety of CAP, respectively (Fig. 2; Table 1), which resulted in *N*-demethylation or methylphenyl hydroxylation, respectively (Fig. 3). Based on these comparisons, it was predicted that the capability differences of P450 proteins to metabolize CAP were in the order CYP6CV5, CYP9A68, CYP321F3, and CYP324A12, further providing a theoretical model for *in vitro* metabolism in P450 functional studies.

3.3. Expression of recombinant P450 proteins

The double-enzyme digestion reaction showed that CYP6CV5, CYP324A1, CYP321F3, CYP9A68, and CPR were connected to the pFastBac1 vector, and the insertion lengths of these P450 genes were 1575, 1506, 1395, 1611, and 2124 bp, respectively (Fig. S1A; Table S1). To detect whether Bacmid DNA completed transposition in DH10Bac, PCR was used to analyze the bacterial colony. As shown in Fig. S1B, the

fragment length of the transposed P450 bacmid DNAs ranged from 3500 to 4500 bp, and the amplification products of those without transposition were 250 bp in size, suggesting that the plasmids of pFastBac1 and P450 genes were successfully transfected into DH10Bac containing shuttle vector bacmid. Western blotting using a $6 \times$ His Tag antibody showed that the protein masses of CYP6CV5, CYP324A12, CYP321F3, and CYP9A68 were 62, 53, 52, and 62 kDa, respectively, and CPR had a 78 kDa mass, which was consistent with the predicted amino acid sequences (Xu et al., 2019). The microsomes of P450/CPR prepared from the infected Sf9 cells showed two bright bands, but those from uninfected cells did not (Fig. 4A). The CO difference spectra showed that the four expressed P450 proteins had a distinct peak at 450 nm after reduction by sodium dithionite and binding of CO, which is a feature of a functioning P450 (Fig. 4B). These results indicated that the four P450 genes were successfully expressed in Sf9 cells using the baculovirus expression system.

3.4. Activity differences of recombinant P450s on model substrates

To determine whether the recombinant P450s were folded correctly *in vitro*, their activities were tested on four fluorescent model substrates. In the EC substrate group, the activities of CYP6CV5 and CYP324A12 (0.54 and 0.46 pmol/min/pmol P450, respectively) were significantly higher than those of CYP9A68 and CYP321F3 (0.37 and 0.35 pmol/min/pmol P450, respectively), and the CYP6CV5 and CYP324A12 activities differed significantly ($F_{1,4} = 96.00$, $P = 0.0006$). CYP6CV5, CYP324A12, CYP321F3, and CYP9A68 could catalyze MR with 0.17, 0.18, 0.16, 0.19 pmol/min/pmol P450 activities, respectively; however, no significant differences were observed among them ($F_{3,8} = 1.76$, $P = 0.2329$). For the EFC substrate, CYP321F3 had the highest activity (0.57 pmol/min/pmol P450), followed by CYP6CV5 and CYP9A68 (0.42 and 0.41 pmol/min/pmol P450, respectively); CYP324A12 had the least activity (0.34 pmol/min/pmol P450) ($F_{3,8} = 433.67$, $P = 0.0001$). CYP6CV5, CYP324A12, CYP321F3, and CYP9A68 metabolized BFC at rates of 0.23, 0.21, 0.38, and 0.67 pmol/min/pmol P450, respectively, indicating that CYP9A68 had the highest activity with BFC as the substrate ($F_{3,8} = 2012.46$, $P = 0.0001$) (Fig. 5). The four recombinant P450 proteins exhibited significantly different activities on fluorescent model substrates and could be used for CAP metabolism.

3.5. Metabolic differences of recombinant P450s to CAP

The metabolic abilities of recombinant P450s to CAP were assessed by investigating the enzyme reactions catalyzing CAP depletion. Primary mass spectrometry showed that CAP could stably ionize to produce $[M + H]^+$ excimer ions $m/z = 483.75$ (Fig. 6A), and the secondary mass spectrometry produced specific fragments with $m/z = 285.77/452.91$ (Fig. 6B). The mother ion $m/z = 483.75$ and the highest abundance daughter ion $m/z = 285.77$ were selected as the daughter and mother ion pair of the MRM for the quantitative CAP test (Table S2). The retention time of CAP was 1.41 min (Fig. 6C). As shown in Fig. 6D, the recovery rates of CAP were 15.86, 50.42, 35.19, 24.37, and 100 % in samples with CYP6CV5, CYP324A12, CYP321F3, CYP9A68, and untransfected Sf9 cell (CK), respectively, and the metabolic rates of these recombinant P450s were 0.97, 0.55, 0.75, and 0.86 pmol/min/pmol P450, respectively, suggesting that the metabolic ability differences of these P450 proteins on CAP were significant ($F_{4,10} = 5580.06$, $P = 0.0001$; $F_{3,8} = 7,157,439.26$, $P = 0.0001$). The rate of CAP reduction in response to CAP concentration revealed Michaelis-Menten kinetics (Fig. S2), and the kinetic parameters of CYP6CV5, CYP324A12, CYP321F3, and CYP9A68 were determined (Table 2): $K_m = 5.6$, 18.4, 10.2, and 7.7 μ M; $V_{max} = 2.5$, 3.2, 3.0, and 2.8 pmol CAP/min/pmol P450. Therefore, the metabolic efficiency (V_{max}/K_m) of CYP6CV5 exhibited the highest value (0.45), followed by that of CYP9A68 (0.37), CYP321F3 (0.30), and CYP324A12 (0.17). These *in vitro* metabolism results indicate that the four P450 proteins can catalyze the oxidation of

Table 1
Molecular docking of the striped rice borer four P450 homology models.

Protein	Insecticide	Estimated free energy (kcal/mol)	Distance
CYP6CV5	Chlorantraniliprole	-7.5	2.9
CYP324A12	Chlorantraniliprole	-7.1	5.1
CYP321F3	Chlorantraniliprole	-7.3	4.3
CYP9A68	Chlorantraniliprole	-7.4	4

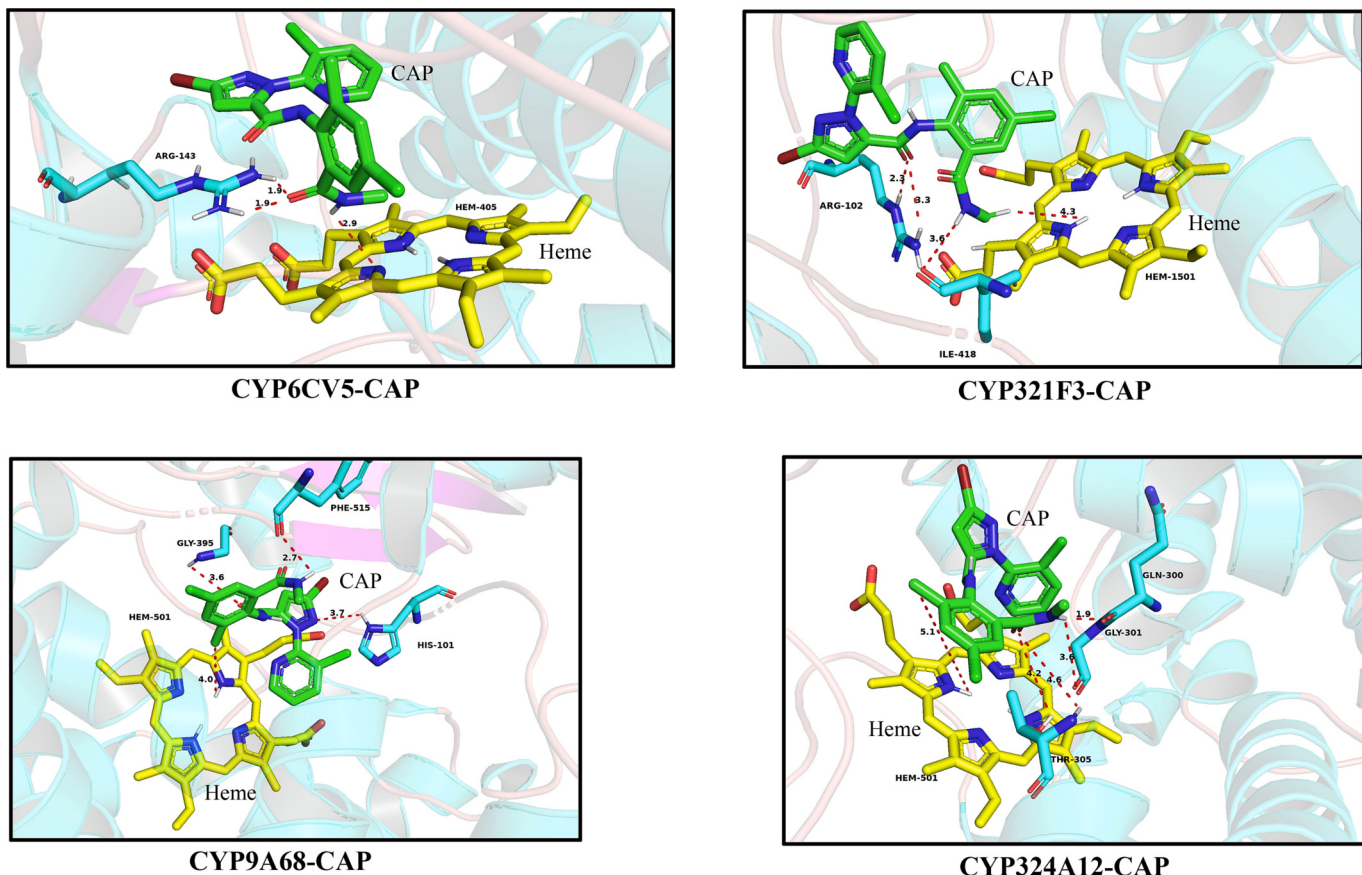


Fig. 2. Molecular docking of P450 homology models with chlorantraniliprole (CAP). CAP indicates as green sticks. Heme is displayed as yellow carbon and blue nitrogen atoms.

CAP, providing vital functional evidence for metabolic differences in P450-mediated metabolic resistance at the protein level.

4. Discussion

CAP (group 28-ryanodine receptor modulators) has been registered for the management of Lepidoptera pests in agricultural crops (such as rice, fruit trees, vegetables, and cotton) in China since 2008 (Yin et al., 2023). Owing to its high activity and rapid action, CAP is extensively used as a reduced-risk insecticide to replace neonicotinoids, organophosphates, carbamates, and pyrethroid insecticides (Rodrigues et al., 2015). However, low-to-moderate levels of CAP resistance in SSB (5.7–21.7-fold) in China were first detected in 2010 (Su et al., 2014), and resistance severity continued to increase in China in the following years (Fig. S3), reaching ratios of 2087.5-fold by 2019 (Huang et al., 2020, 2021). The development of CAP resistance will cause a significant increase in usage for better control of SSB. In addition, Chinese farmers frequently exceed the recommended dosage when spraying insecticides (Wu et al., 2018a). Therefore, the actual initial CAP concentration in the environments may be higher than expected. Moreover, inadequate field control and CAP resistance-induced excessive use further facilitate the development of CAP resistance into a malignant status, causing environmental pollution and affecting the safety of human health (Khan et al., 2021). Previous studies have indicated that approximately 10 % of sprayed CAP adheres to plants, with only 0.1 % reaching target pests, leading to a low CAP efficiency (Yin et al., 2023; Zong et al., 2023). Therefore, a large proportion of CAP enters the soil and water, and CAP residues tend to accumulate in edaphic and aquatic environment due to its persistence and mobility (Wang et al., 2021), posing toxicity effects to non-target organisms such as honeybees, silkworms, natural enemies,

fishes, mammals, and soil invertebrates (Ibrahim et al., 2020b; Ibrahim et al., 2021; Khan et al., 2021; Liu et al., 2018; Liu et al., 2023; Yin et al., 2023; Zhu et al., 2023). Exposure to CAP adversely influences the development, reproduction, survival, physiology, and biochemical and molecular parameters of non-target insects (Khan et al., 2021; Liu et al., 2018; Liu et al., 2023; Zhu et al., 2023); therefore, the safety of its use in integrative pest management should be considered. The current study represents our effort to track and predict resistance spread via insights into the novel molecular mechanisms of CAP resistance episodes (Richardson et al., 2020), which will provide effective resistance management measures for eliminating CAP toxicity risks to ecosystems (Teixeira and Andaloro, 2013).

Insecticides are broken down into non-toxic forms through multiple biotransformation pathways within the Phase I (P450 and EST) and II (GST and UGT) enzyme systems. The products of Phase I reactions often become the substrates of Phase II enzymes, which together enable the export of compounds from the body; for instance, water-soluble compounds are then transferred and excreted by ABC transporters during Phase III (Amezian et al., 2021b; Perry et al., 2011) (Fig. 7). Metabolic resistance is a common and serious threat to CAP efficacy. Cytochrome P450s are the primary detoxification enzymes associated with metabolic resistance to many synthetic insecticides (Lu et al., 2021). The constitutive overexpression of P450 genes is a common phenomenon in insecticide-resistant strains and has been found in many resistant insect species. In imidacloprid-resistant *Nilaparvata lugens*, the overexpression of *CYP6AY1*, *CYP6ER1*, *CYP4CE1*, and *CYP6CW1* was reported (Zhang et al., 2016). The co-upregulation of six P450 genes, *CYP4M6*, *CYP4M7*, *CYP6AE11*, *CYP9A12*, *CYP332A1*, and *CYP337B1*, was observed in deltamethrin-resistant *Helicoverpa armigera* (Brun-Barale et al., 2010). Multiple P450 genes (*CYP6CY13*, *CYP6CY19*, *CYP6CY4*, *CYP6CY18*,

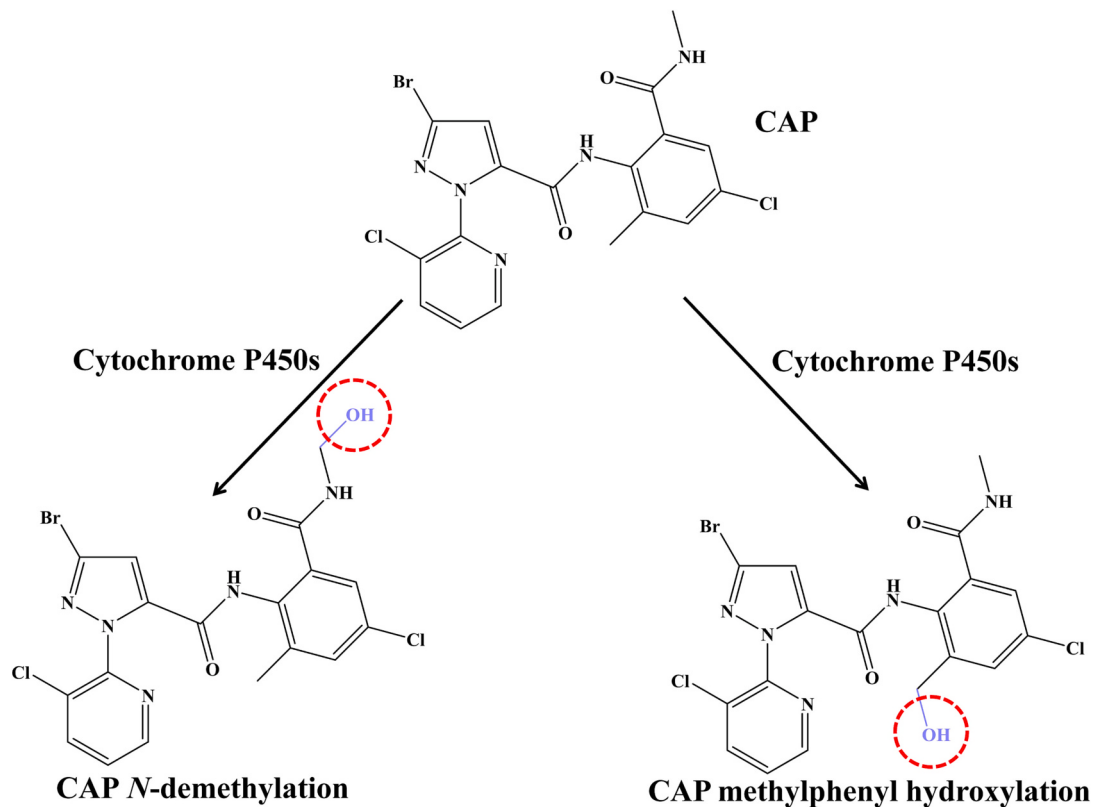


Fig. 3. Hydroxylation sites (in red circle) of chlorantraniliprole (CAP) catalyzed by the recombinant P450s via computational molecular modeling simulation suggesting methylphenyl hydroxylation and N-demethylation.

CYP4CJ1, *CYP6A2*, *CYP6J1*, *CYP380C6M*, and *CYP3323A1*) were constitutively overexpressed in a sulfoxoeflor-resistant strain of *Aphis gossypii* (Ma et al., 2019). These results suggest a link between the overexpression of P450 genes and insecticide resistance (Lu et al., 2021). However, a notable characteristic of insect P450s is that its metabolic resistance is associated with increased protein activities through the transcriptional upregulation of its genes in resistant strains (Liu et al., 2015). Therefore, the overexpression of P450 genes in insecticide-resistant insects might not be associated with insecticide resistance. Our previous study showed that *CYP6CV5*, *CYP9A68*, *CYP321F3*, and *CYP324A12* were constitutively overexpressed in CAP-resistant strains of SSB, all of which belong to the CYP3 clan. Insect P450s are generally classified into four clans: CYP2, CYP3, CYP4, and the mitochondrial P450s. Of these, the CYP3 clan is a large group of P450s, comprising the *CYP3*, *CYP5*, *CYP6*, *CYP9*, *CYP28*, *CYP308-310*, *CYP317*, *CYP321*, *CYP324*, *CYP329*, *CYP332*, *CYP336-338*, and *CYP345-348* subfamilies (Amezian et al., 2021a), which are primarily involved in insecticide resistance and metabolism. Thus, we performed a functional study to compare the capabilities of *CYP6CV5*, *CYP9A68*, *CYP321F3*, and *CYP324A12* from the CYP3 clan to metabolize CAP in SSB, providing a functional link between genotype and phenotype.

In this study, we report for the first time that *CYP6CV5*, *CYP9A68*, *CYP321F3*, and *CYP324A12* were successfully heterologously expressed in Sf9 cells using a baculovirus expression system. Sf9 cells from *S. frugiperda* have been successfully used as a system for the heterologous expression of P450 proteins (Amezian et al., 2022), and the baculovirus expression system is an efficient tool for studying gene function and has been used to study insecticide metabolic resistance mechanisms (Nauen et al., 2021). In this system, after introducing the enzyme cleavage site, the target gene is first incorporated into the pFastBac vector to construct a recombinant plasmid, which is transformed into DH10Bac competent cells carrying the viral shuttle vector bacmid. We identified the sequence information of *CYP6CV5*, *CYP9A68*,

CYP321F3, and *CYP324A12* by aligning the SSB genome. The four P450 genes in the CYP3 clan were mapped to their four chromosomes and had different numbers of exons and introns, suggesting the integrity and credibility of these four P450 sequences. In *H. armigera*, the sequence analysis of *CYP6AEs* has been performed at the genomic level before heterologous expression (Shi et al., 2018). Therefore, the integrity and accuracy of the target gene transcript sequences are crucial factors for ensuring successful heterologous expression. The *CYP6*, *CYP9*, *CYP321*, and *CYP324* subfamilies in the CYP3 clan had reportedly expanded as an evolutionary requirement in the genome, allowing them to tolerate xenobiotics (Amezian et al., 2021a; Heidel-Fischer and Vogel, 2015). Notably, *CYP6CV5*, *CYP9A68*, *CYP321F3*, and *CYP324A12* transcriptional responses can inferably match their metabolic capacities, highlighting their roles in CAP resistance in SSB (Nauen et al., 2021).

Our study showed the co-expression of P450s and CPR in Sf9 cells using the baculovirus system. CPR is required for electron transfer from NADPH to P450 proteins to catalyze the monooxygenase reactions (Nauen et al., 2021). Therefore, CPR has been used as an electron transporter for P450 functional expression *in vitro*, including in *Laodelphax striatellus* *CYP6AY3v2* and *CYP353D1v2* (Elzaki et al., 2017; Wang et al., 2017), *Apis mellifera* *CYP9Q2* and *CYP9Q3* (Haas et al., 2022), and *H. armigera* *CYP6AEs* (Shi et al., 2018). In the baculovirus expression system, the MOI ratio of the recombinant P450 and CPR viruses influences the catalytic efficiency of the recombinant P450 protein on the substrate. If the MOI ratio of the recombinant virus with P450 and CPR is 1:1, the activity value of the P450 enzyme is the highest; however, the P420 proportion in the microsomes increases accordingly. P420 is an inactivated P450 enzyme that critically affects P450 enzyme activity. We adopted an MOI ratio of 2:0.2 for recombinant P450 and CPR virus, and the metabolic rates of *CYP6CV5*, *CYP324A12*, *CYP321F3*, and *CYP9A68* were 0.97, 0.55, 0.75, and 0.86 pmol/min/pmol P450, respectively. This result indicates that the present MOI ratio did not weaken the metabolic abilities of these four recombinant P450s,

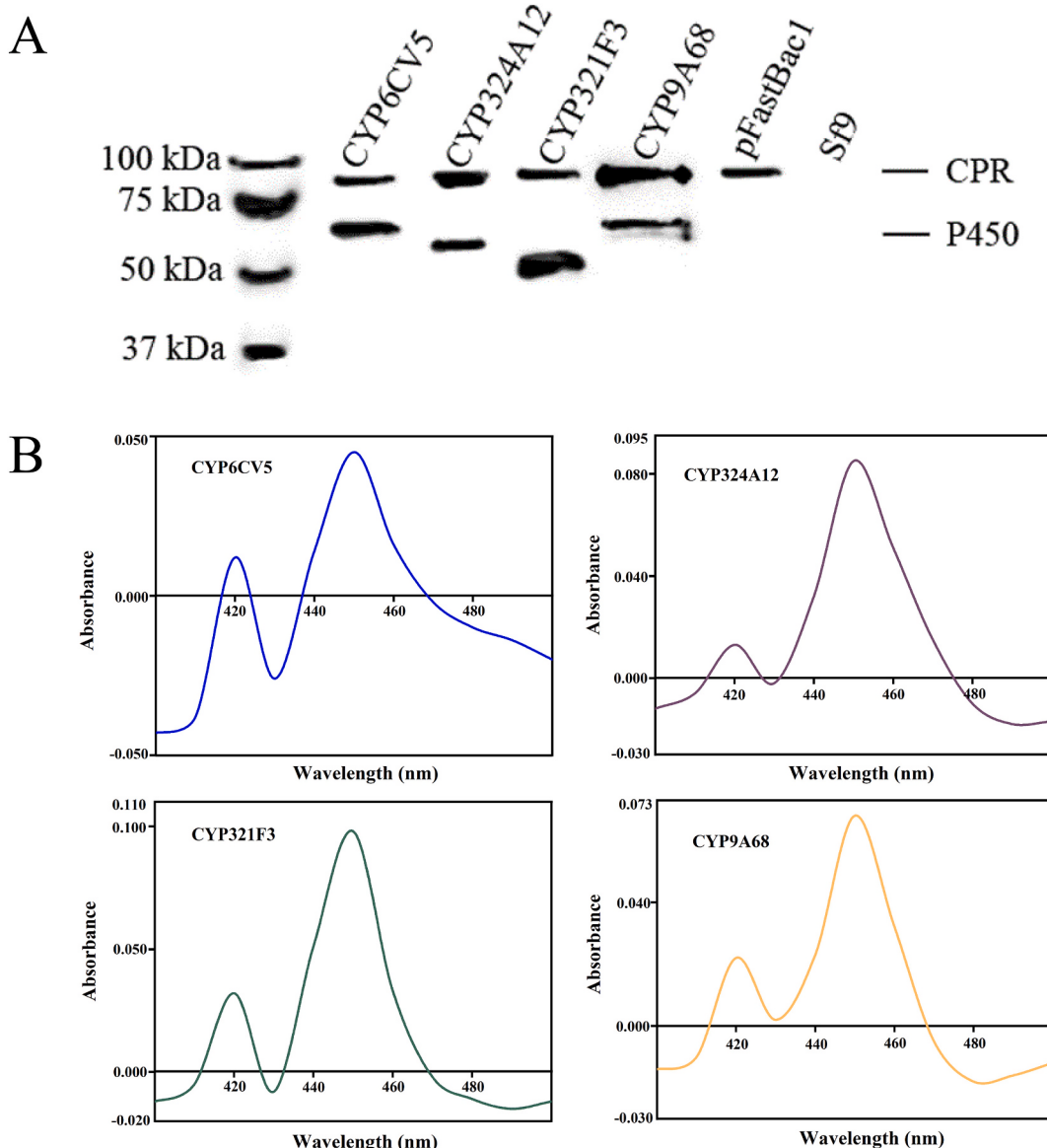


Fig. 4. Heterologous expression of the striped rice borer *CYP6CV5*, *CYP324A12*, *CYP321F3*, and *CYP9A68*. A. Western blotting detection of the recombinant P450s and CPR protein in microsomes. Sf9 insect cells only infected with non-insertion virus are used as negative controls. B. Reduced carbon monoxide (CO) difference spectra of the recombinant P450s.

although P420s existed in the P450/CPR microsomes according to the reduced CO difference spectrum assay (Fig. 4B). Similar MOI ratios have been reported in *H. armigera* (Shi et al., 2018) and *S. exigua* (Hu et al., 2020). In addition, quantitative real-time PCR analysis showed the expression levels of *CYP6CV5*, *CYP9A68*, *CYP321F3*, and *CYP324A12* were 13.14-, 44.88-, 6.63-, and 4.48-fold, respectively, in the CAP-selected resistant SSB strains (Xu et al., 2019). Thus, it is interesting to find out the importance of these four P450 gene/proteins in CAP resistance in SSB, from CAP metabolic efficiencies through heterologous functional expression.

We used different fluorescent P450 model substrates to probe the four recombinant P450 activities. In this study, four substrates were tested, and the results showed that *CYP6CV5*, *CYP324A12*, *CYP321F3*, and *CYP9A68* had high activities toward EC, EC, EFC, and BFC, respectively, suggesting their preference for O-dealkylation and O-debenzylation reactions. Our findings are similar to those of P450 activity reactions in *Bemisia tabaci* (Karunker et al., 2009) and *S. frugiperda* (Amezian et al., 2022). These results reveal that not all fluorescent model substrates are suitable diagnostic probes for P450s. Thus, a

fluorescent model substrate should be selected to probe the specific P450 activity. The heterologous expression of P450 facilitates the screening of specific diagnostic probes using specific enzyme activity tests. These four P450 proteins exhibited significant metabolic differences to their fluorescent substrates. To support the metabolic competence differences of recombinant P450s in the CAP resistance of SSB, the interactions between these four P450s and CAP were first elucidated using computational molecular modeling simulation. CAP was docked into the active center hemes of *CYP6CV5*, *CYP324A12*, *CYP321F3*, and *CYP9A68* at different free energies and distances. Cytochrome P450 is a monooxygenase that catalyzes the transfer of oxygen atoms, with mercaptan combined with heme as the active center that inserts heme-activated oxygen into the oxidation site of the substrate to oxidize it. Smaller free-energy values and shorter docking distances represented greater combination and attack capabilities, indicating that *CYP6CV5* had the strongest capability to metabolize CAP compared with *CYP324A12*, *CYP321F3*, and *CYP9A68*. Therefore, this analysis suggests that these four P450s have significant metabolic differences on CAP. The binding of these four P450s to CAP isolates it, preventing or delaying its

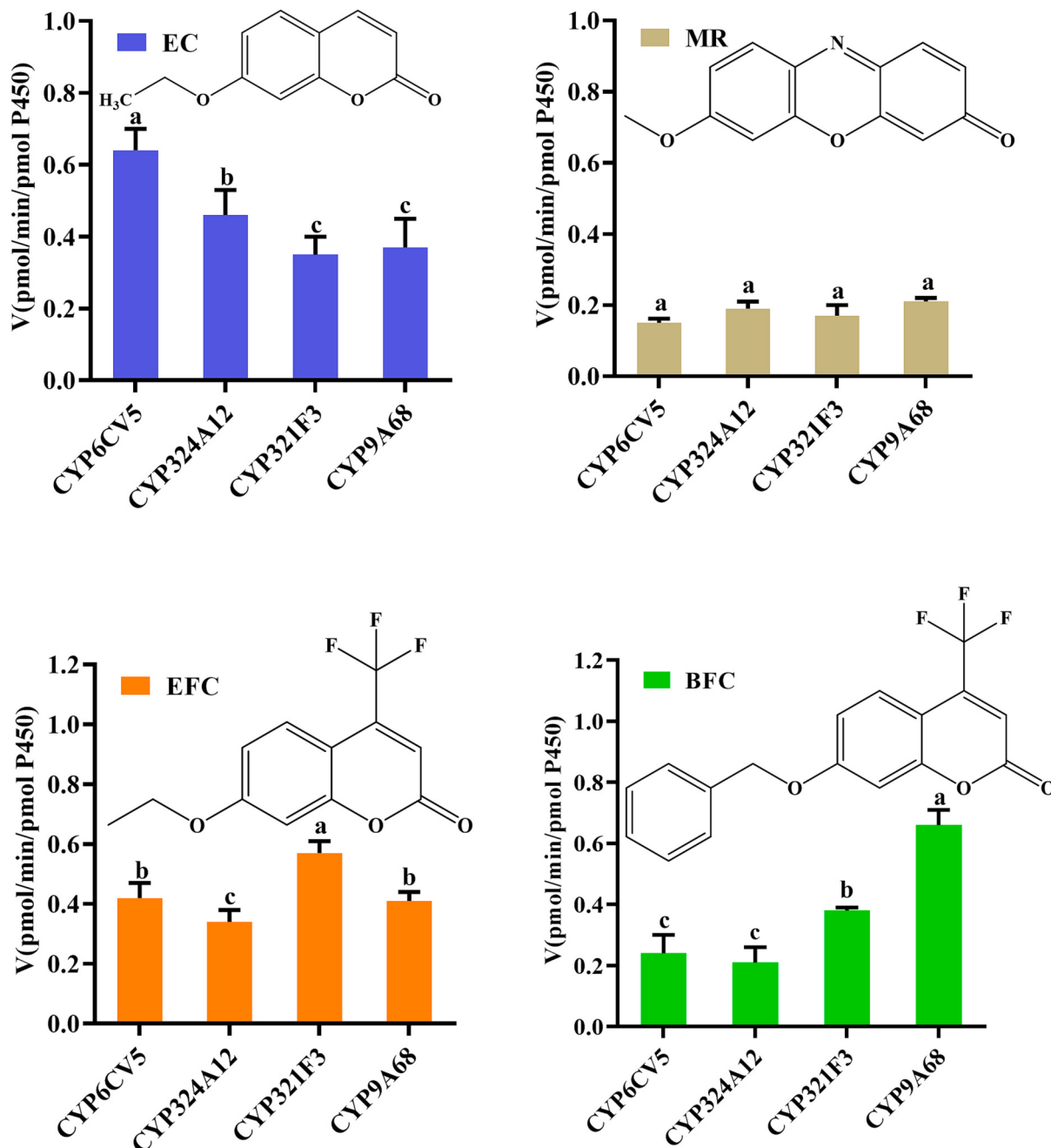


Fig. 5. Metabolism of four fluorescent P450 model substrates by the recombinant CYP6CV5, CYP324A12, CYP321F3, and CYP9A68. Error bars represent the SD from the mean of three independent replicates (different letters indicate significant differences among treatments as determined using one-way ANOVA followed by Tukey's HSD test ($P < 0.05$)).

action on RyRs, causing the development of SSB metabolic resistance (Perry et al., 2011). These four P450s preferred docking the antraniloyl moiety of CAP with either the *N*-methyl carbon or the methylphenyl. A recent study reported that CAP is hydroxylated at sites of the *N*-methyl carbon and the methylphenyl to generate *N*-demethylation and methylphenyl hydroxylation in *A. mellifera* (Haas et al., 2022). A hydroxylation event is a common type of P450 catalytic oxidation reaction of insecticides. Examples include CYP6CM1vQ in *B. tabaci* (Karunker et al., 2009), CYP6ER1 and CYP6AY1 in *N. lugens* (Ding et al., 2013; Zimmer et al., 2018), CYP6AY3v2, CYP353D1v2, CYP6FU1, and CYP439A1v3 in *L. striatellus* (Elzaki et al., 2017; Elzaki et al., 2018; Miah et al., 2019; Wang et al., 2017), and CYP6AEs in *H. armigera* (Shi et al., 2018). Therefore, hydroxylation may be a potential mechanism for CAP metabolism in SSB (Katsavou et al., 2022).

Furthermore, we utilized UPLC-MS-targeted detection of CAP disappearance to compare the metabolic abilities of CYP6CV5, CYP324A12, CYP321F3, and CYP9A68 on CAP, as CAP has many oxidative products, most of which are commercially unavailable. Our results demonstrate that CYP6CV5, CYP324A12, CYP321F3, and CYP9A68 can metabolize CAP, while highlighting significant variations in the metabolic efficiency of CAP. The metabolic efficiency (V_{max}/K_m) of CYP6CV5, CYP324A12, CYP321F3, and CYP9A68 showed significant variations with different K_m and V_{max} values to CAP. The K_m value reflects the affinity between P450 and CAP. Therefore, it can be inferred that all four P450s have high affinities toward CAP compared to other insects' P450 (Elzaki et al., 2017; Karunker et al., 2009; Shi et al., 2018; Wang et al., 2017). These results provide direct evidence to confirm that these four overexpressed P450 genes jointly confer CAP resistance in

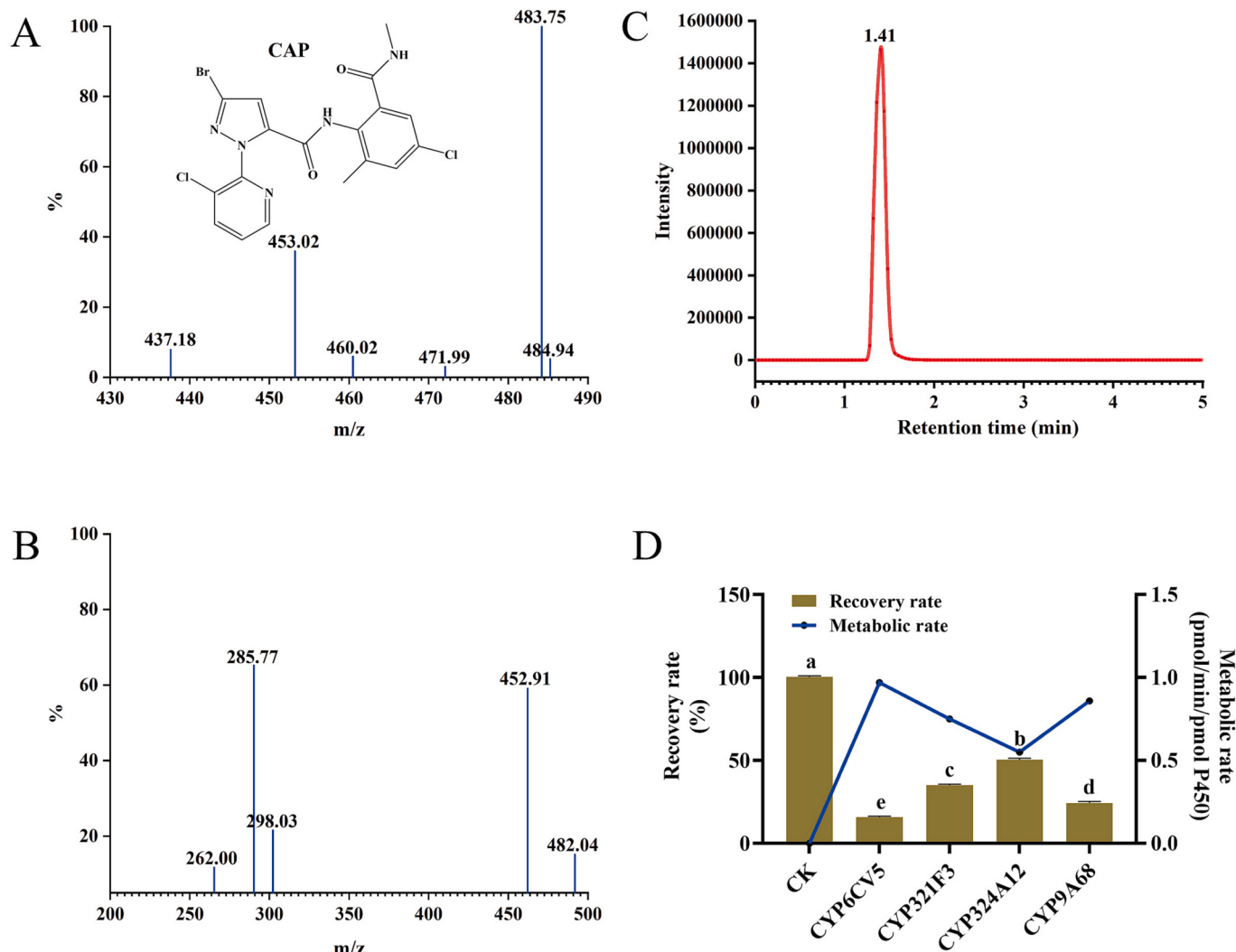


Fig. 6. Metabolic detection of chlorantraniliprole (CAP) using ultra high performance liquid chromatography mass spectrometry. A. Primary mass spectrometry of CAP. B. Secondary mass spectrometry of CAP. C. Multiple reaction monitoring spectrum of CAP. D. Recovery rates and metabolic rates of CAP. Error bars represent the SD from the mean of three independent replicates (different letters indicate significant differences among treatments as determined using one-way ANOVA followed by Tukey's HSD test ($P < 0.05$)).

Table 2
Kinetic parameters of the striped rice borer four P450s with chlorantraniliprole.

Enzyme	V_{max} (pmol CAP/min/pmol P450)	K_m (μM)	Clearance (V_{max}/K_m)
CYP6CV5	2.5	5.6	0.45
CYP324A12	3.2	18.4	0.17
CYP321F3	3.0	10.2	0.30
CYP9A68	2.8	7.7	0.37

SSB. Further studies are required to identify the primary metabolites after CAP incubations with CYP6CV5, CYP324A12, CYP321F3, and CYP9A68. To our knowledge, this is the first study that provides functional evidence of CAP metabolic resistance mediated by multiple P450s from the CYP3 clan at the protein level. Therefore, based on new insights from the current study, sensitive molecular diagnostic markers can be feasibly developed to monitor CAP metabolic resistance and make decisions on CAP use in time and space in the field. Due to concerns on environmental pollution and human health concerns, the application of molecular markers is of great value for insecticide resistance management when crop protection policies will rely on a “last resort” chemical control (Leeuwen et al., 2020). Moreover, new control technologies

targeting these P450s can also be developed for field applications. On the basis of P450 sequence information, double-stranded ribonucleic acid (dsRNA) is designed to develop nano-insecticides and genetically modified crops containing dsRNA, and insecticidal compounds with high activity, high affinity, and high selectivity can also be designed and synthesized. These techniques targeting P450s can successfully control the population of pests in the field, thereby reducing in insecticide use and environmental risk.

5. Conclusions

This study provides the first insights into the molecular metabolic resistance mechanisms of SSB for CAP metabolism using multiple P450 proteins isolated from a CAP-selected strain. CYP6CV5, CYP324A12, CYP321F3, and CYP9A68 can metabolize CAP at different rates, suggesting that these four P450s function efficiently through a joint mode of action in CAP metabolic resistance. Enzyme activity analysis showed that these four P450s preferred different fluorescent model probe substrates, suggesting that potentially specific diagnostic probes could be developed as biomarkers for detecting environmental pollution from CAP. In this case study, the overexpression level differences of these four P450 genes did not positively correspond to the metabolic differences of

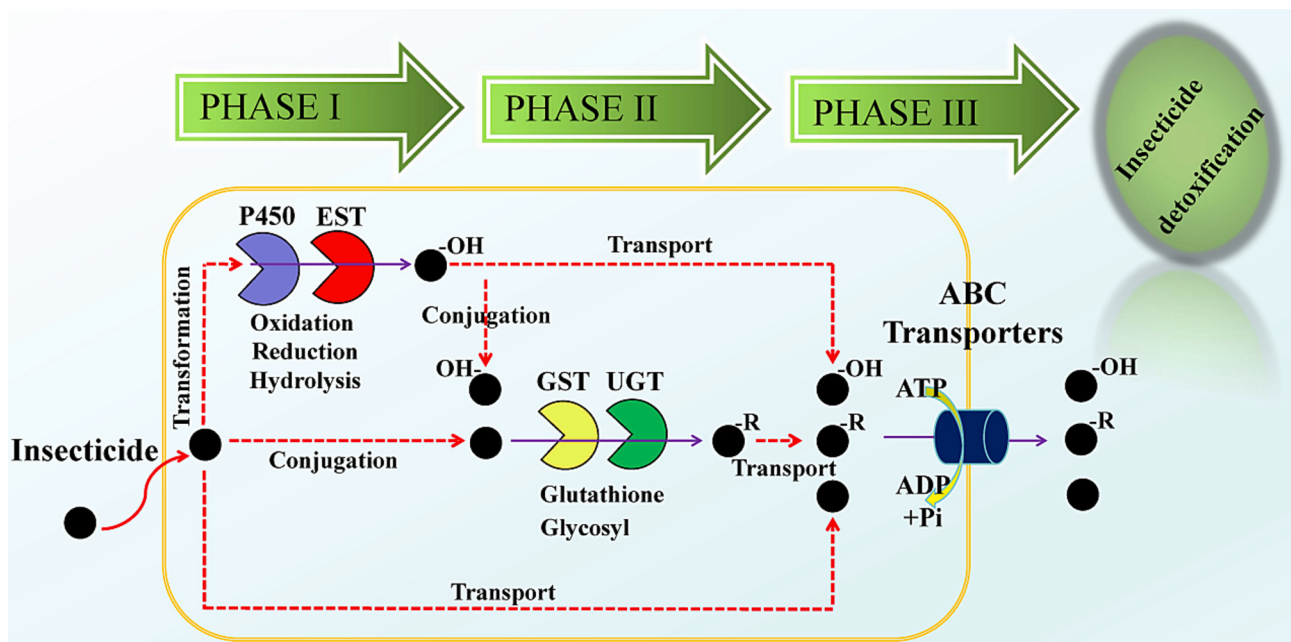


Fig. 7. General model diagram involving different metabolic pathways of insecticide detoxification in the striped rice borer. Phase I enzymes including P450 and EST perform oxidation, reduction, or hydrolysis reactions. Phase II enzymes such as GST and UGT add glutathione and glycosyl groups to the products of Phase I reactions. ABC transporters in phase III transport the polar compounds or conjugates or toxicants without enzymatic modifications out of the cell. The simultaneous operation of Phase I, II, and III pathways is displayed. ABC: adenosine triphosphate-binding cassette transporter. ATP: adenosine triphosphate. ADP: adenosine diphosphate. Pi: phosphate radical.

their recombinant proteins on CAP, indicating that uncovering the significance of P450s as “ready to use” genes in insecticide metabolic resistance is reasonable based on the expression quantities combined with the metabolic rates of heterologously expressed proteins. Our findings enhance the understanding of resistance management strategies and can be used to assist in hazard and risk assessments for the environmental management of CAP.

CRediT authorship contribution statement

Lu Xu: Conceptualization, Funding acquisition, Methodology, Project administration, Resources, Visualization, Writing – original draft, Writing – review & editing. **Jun Zhao:** Data curation, Funding acquisition, Investigation. **Dejin Xu:** Funding acquisition, Software. **Guang-chun Xu:** Validation. **Yingchuan Peng:** Data curation, Funding acquisition, Software. **Yanan Zhang:** Project administration, Resources, Supervision.

Declaration of competing interest

The authors declare that they have no known competing financial interests or personal relationships that could have appeared to influence the work reported in this study.

Data availability

Data will be made available on request.

Acknowledgments

This study was supported by the National Natural Science Foundation of China (grant number: 31972309) and the Special Fund Project for Basic Scientific Research Business of the Jiangsu Academy of Agricultural Sciences (grant number: ZX(22)413) and the Anhui Province University Natural Science Research Outstanding Youth Project (grant number: 2023AH020040) and the Natural Science Foundation of

Jiangxi Province (grant number: 20224BAB215019) and the Independent Innovation Project of Henan Academy of Agricultural Sciences (grant number: 2023ZC024) and the Jiangsu Agriculture Science and Technology Innovation Fund (grant number: CX(22)2038).

Appendix A. Supplementary data

Supplementary data to this article can be found online at <https://doi.org/10.1016/j.scitotenv.2023.169229>.

References

- Amezian, D., Nauen, R., Goff, G.L., 2021a. Comparative analysis of the detoxification gene inventory of four major *Spodoptera* pest species in response to xenobiotics. *Insect Biochem. Mol. Biol.* 138, 103646.
- Amezian, D., Nauen, R., Goff, G.L., 2021b. Transcriptional regulation of xenobiotic detoxification genes in insects—an overview. *Pestic. Biochem. Physiol.* 174, 104822.
- Amezian, D., Mehlhorn, S., Vacher-Chicane, C., Nauen, R., Goff, G.L., 2022. *Spodoptera frugiperda* Sf9 cells as a model system to investigate the role of detoxification gene expression in response to xenobiotics. *Curr. Opin. Insect Sci.* 2, 100037.
- Bass, C., Nauen, R., 2023. The molecular mechanisms of insecticide resistance in aphid crop pests. *Insect Biochem. Mol. Biol.* 156, 103937.
- Brun-Barale, A., Hema, O., Martin, T., Suraporn, S., Audant, P., Sezutsu, H., Feyerisen, R., 2010. Multiple P450 genes overexpressed in deltamethrin-resistant strains of *Helicoverpa armigera*. *Pest Manag. Sci.* 66, 900–909.
- Ding, Z.P., Wen, Y.C., Yang, B.J., Zhang, Y.X., Liu, S.H., Liu, Z.W., Han, Z.J., 2013. Biochemical mechanisms of imidacloprid resistance in *Nilaparvata lugens*: over-expression of cytochrome P450 CYP6AY1. *Insect Biochem. Mol. Biol.* 43, 1021–1027.
- Elzaki, M.E.A., Miah, M.A., Wu, M., Zhang, H.M., Pu, J., Jiang, L., Han, Z.J., 2017. Imidacloprid is degraded by CYP353D1v2, a cytochrome P450 overexpressed in a resistant strain of *Laodelphax striatellus*. *Pest Manag. Sci.* 73, 1358–1363.
- Elzaki, M.E.A., Miah, M.A., Peng, Y.C., Zhang, H.M., Jiang, L., Wu, M., Han, Z.J., 2018. Deltamethrin is metabolized by CYP6FU1, a cytochrome P450 associated with pyrethroid resistance, in *Laodelphax striatellus*. *Pest Manag. Sci.* 74, 1265–1271.
- Ferreira, P., Gabriel, A., Sousa, J.P., Natal-da-Luz, T., 2022. Representativeness of *Folsomia candida* to assess toxicity of a new generation insecticide in different temperature scenarios. *Sci. Total Environ.* 837, 155712.
- Haas, J., Glaubitz, J., Koenig, U., Nauen, R., 2022. A mechanism-based approach unveils metabolic routes potentially mediating chlorantraniliprole synergism in honey bees, *Apis mellifera* L., by azole fungicides. *Pest Manag. Sci.* 78, 965–973.
- Heidel-Fischer, H.M., Vogel, H., 2015. Molecular mechanisms of insect adaptation to plant secondary compounds. *Curr. Opin. Insect Sci.* 8, 8–14.

- Hu, Z.D., Lin, Q.S., Chen, S.H., Li, Z.Y., Yin, F., Feng, X., 2014. Identification of a novel cytochrome P450 gene, *CYP321E1* from the diamondback moth, *Plutella xylostella* (L.) and RNA interference to evaluate its role in chlorantraniliprole resistance. *Bull. Entomol. Res.* 104, 716–723.
- Hu, B., Ren, M.M., Fan, J.F., Huang, S.F., Wang, X., Elzaki, M.E.A., Bass, C., Palli, S.R., Su, J.Y., 2020. Xenobiotic transcription factors CncC and maf regulate expression of *CYP321A16* and *CYP332A1* that mediate chloryrifos resistance in *Spodoptera exigua*. *J. Hazard. Mater.* 398, 122971.
- Huang, J.M., Rao, C., Wang, S., He, L.F., Zhao, S.Q., Zhou, L.Q., Zhao, Y.X., Yang, F.X., Gao, C.F., Wu, S.F., 2020. Multiple target-site mutations occurring in lepidopterans confer resistance to diamide insecticides. *Insect Biochem. Mol. Biol.* 121, 103367.
- Huang, J.M., Sun, H., He, L.F., Liu, C., Ge, W.C., Ni, H., Gao, C.F., Wu, S.F., 2021. Double ryanodine receptor mutations confer higher diamide resistance in rice stem borer, *Chilo suppressalis*. *Pest Manag. Sci.* 77, 4971–4979.
- Ibrahim, K.A., Abdelgaid, H.A., El-Dessouky, M.A., Fahmi, A.A., Abdel-Daim, M.M., 2020a. Modulation of paraoxonase-1 and apoptotic gene expression involves in the cardioprotective role of flaxseed following gestational exposure to diesel exhaust particles and/or fenitrothion insecticide. *Cardiovasc. Toxicol.* 20, 604–617.
- Ibrahim, K.A., Eleyan, M., El-Rahman, H.A.A., Khwanes, S.A., Mohamed, R.A., 2020b. Quercetin attenuates the oxidative injury—mediated upregulation of apoptotic gene expression and catecholaminergic neurotransmitters of the fetal rats' brain following prenatal exposure to fenitrothion insecticide. *Neurotox. Res.* 37, 871–882.
- Ibrahim, K.A., Abdelgaid, H.A., El-Dessouky, M.A., Fahmi, A.A., Abdel-Daim, M.M., 2021. Linseed ameliorates renal apoptosis in rat fetuses induced by single or combined exposure to diesel nanoparticles or fenitrothion by inhibiting transcriptional activation of p21/p53 and caspase-3/9 through pro-oxidant stimulus. *Environ. Toxicol.* 36, 958–974.
- Ibrahim, K.A., Abdelgaid, H.A., Eleyan, M., Mohamed, R.A., Gamil, N.M., 2022. Resveratrol alleviates cardiac apoptosis following exposure to fenitrothion by modulating the sirtuin1/c-Jun N-terminal kinases/p53 pathway through pro-oxidant and inflammatory response improvements: in vivo and in silico studies. *Life Sci.* 290, 120265.
- Ju, D., Mota-Sanchez, D., Fuentes-Contreras, E., Zhang, Y.L., Wang, X.Q., Yang, X.Q., 2021. Insecticide resistance in the *Cydia pomonella* (L): global status, mechanisms, and research directions. *Pestic. Biochem. Physiol.* 178, 104925.
- Karunker, I., Morou, E., Nikou, D., Nauen, R., Sertchook, R., Stevenson, B.J., Paine, M.J., Morin, S., Vontas, J., 2009. Structural model and functional characterization of the *Bemisia tabaci* CYP6CM1vQ, a cytochrome P450 associated with high levels of imidacloprid resistance. *Insect Biochem. Mol. Biol.* 39, 697–706.
- Katsavou, E., Riga, M., Ioannidis, P., King, R., Zimmer, C.T., Vontas, J., 2022. Functionally characterized arthropod pest and pollinator cytochrome P450s associated with xenobiotic metabolism. *Pestic. Biochem. Physiol.* 181, 105005.
- Khan, M.M., Hafeez, M., Elgizawy, K., Wang, H.Y., Zhao, J., Cai, W.L., Ma, W.H., Hua, H.X., 2021. Sublethal effects of chlorantraniliprole on *Paederus fuscipes* (Staphylinidae: Coleoptera), a general predator in paddle field. *Environ. Pollut.* 291, 118171.
- Leeuwen, T.V., Dermauw, W., Mavridis, K., Vontas, J., 2020. Significance and interpretation of molecular diagnostics for insecticide resistance management of agricultural pests. *Curr. Opin. Insect Sci.* 39, 69–76.
- Li, X.X., Li, R., Zhu, B., Gao, X.W., Liang, P., 2018. Overexpression of cytochrome P450 CYP6BG1 may contribute to chlorantraniliprole resistance in *Plutella xylostella* (L.). *Pest Manag. Sci.* 74, 1386–1393.
- Li, W.L., Yang, W., Shi, Y., Yang, X.Y., Liu, S.Q., Liao, X.L., Shi, L., 2024. Comprehensive analysis of the overexpressed cytochrome P450-based insecticide resistance mechanism in *Spodoptera litura*. *J. Hazard. Mater.* 461, 132605.
- Liu, N.N., Li, M., Gong, Y.H., Liu, F., Li, T., 2015. Cytochrome P450s—their expression, regulation, and role in insecticide resistance. *Pestic. Biochem. Physiol.* 120, 77–81.
- Liu, T., Wang, X.G., Chen, D., Li, Y.Q., Wang, F.L., 2018. Growth, reproduction and biochemical toxicity of chlorantraniliprole in soil on earthworms (*Eisenia fetida*). *Ecotoxicol. Environ. Saf.* 150, 18–25.
- Liu, Z.Y., Wu, F.T., Li, F.Q., Wei, Y., 2023. Methionine can reduce the sublethal risk of chlorantraniliprole to honeybees (*Apis mellifera* L.): based on metabolomics analysis. *Ecotoxicol. Environ. Saf.* 268, 115682.
- Lu, K., Song, Y.Y., Zeng, R.S., 2021. The role of cytochrome P450-mediated detoxification in insect adaptation to xenobiotics. *Curr. Opin. Insect Sci.* 43, 103–107.
- Lu, Y.H., Zheng, X.S., He, X.C., Guo, J.W., Fu, Q.M., Xu, H.X., Lu, Z.X., 2023. Sublethal effects of chlorantraniliprole on growth, biochemical and molecular parameters in two chironomids, *Chironomus kienensis* and *Chironomus javanus*. *Ecotoxicol. Environ. Saf.* 253, 114658.
- Ma, K.S., Tang, Q.L., Zhang, B.Z., Liang, P., Wang, B.M., Gao, X.W., 2019. Overexpression of multiple cytochrome P450 genes associated with sulfoxaflo resistance in *Aphis gossypii* glover. *Pestic. Biochem. Physiol.* 157, 204–210.
- Margus, A., Tikka, S., Karvanen, J., Lindström, L., 2024. Transgenerational sublethal pyrethroid exposure gives rise to insecticide resistance in a pest insect. *Sci. Total Environ.* 908, 168114.
- Miah, M.A., Elzaki, M.E.A., Husna, A., Han, Z.J., 2019. An overexpressed cytochrome P450 CYP439A1v3 confers deltamethrin resistance in *Laodelphax striatellus* Fallén (Hemiptera: Delphacidae). *Arch. Insect Biochem. Physiol.* 100, e21525.
- Nauen, R., Zimmer, C.T., Vontas, J., 2021. Heterologous expression of insect P450 enzymes that metabolize xenobiotics. *Curr. Opin. Insect Sci.* 43, 78–84.
- Nauen, R., Bass, C., Feyereisen, R., Vontas, J., 2022. The role of cytochrome P450s in insect toxicology and resistance. *Annu. Rev. Entomol.* 67, 105–124.
- Perry, T., Batterham, P., Daborn, P.J., 2011. The biology of insecticidal activity and resistance. *Insect Biochem. Mol. Biol.* 41, 411–422.
- Richardson, E.B., Troczka, B.J., Gutbrod, O., Davies, T.G.E., Nauen, R., 2020. Diamide resistance: 10 years of lessons from lepidopteran pests. *J. Pest. Sci.* 93, 911–928.
- Rodrigues, A.C.M., Gravato, C., Quintaneiro, C., Golovko, O., Žlábek, V., Barata, C., Soares, A.M.V.M., Pestana, J.L.T., 2015. Life history and biochemical effects of chlorantraniliprole on *Chironomus riparius*. *Sci. Total Environ.* 508, 506–513.
- Roy, A., Kucukural, A., Zhang, Y., 2010. I-TASSER: a unified platform for auto-mated protein structure and function prediction. *Nat. Protoc.* 5, 725–738.
- Shi, Y., Wang, H.D., Liu, Z., Wu, S.W., Yang, Y.H., Feyereisen, R., Heckel, D.G., Wu, Y.D., 2018. Phylogenetic and functional characterization of ten P450 genes from the CYP6AE subfamily of *Helicoverpa armigera* involved in xenobiotic metabolism. *Insect Biochem. Mol. Biol.* 93, 79–91.
- Shi, Y., Sun, S., Zhang, Y.J., He, Y.S., Du, M.H., ÓReilly, A.O., Wu, S.W., Yang, Y.H., Wu, Y.D., 2022. Single amino acid variations drive functional divergence of cytochrome P450s in *Helicoverpa* species. *Insect Biochem. Mol. Biol.* 146, 103796.
- Sparks, T.C., Crossthwaite, A.J., Nauen, R., Banba, S., Cordova, D., Earley, F., Ebbinghaus-Kintzcher, U., Fujioka, S., Hirao, A., Karmon, D., Kennedy, R., Nakao, T., Popham, H.J.R., Salgado, V., Watson, G.B., Wedel, B.J., Wessels, F.J., 2020. Insecticides, biologics and nematicides: updates to IRAC's mode of action classification—a tool for resistance management. *Pestic. Biochem. Physiol.* 167, 104587.
- Su, J.Y., Zhang, Z.Z., Wu, M., Gao, C.F., 2014. Geographic susceptibility of *Chilo suppressalis* Walker (Lepidoptera: Crambidae), to chlorantraniliprole in China. *Pest Manag. Sci.* 70, 989–995.
- Teixeira, L.A., Andaloro, J.T., 2013. Diamide insecticides: global efforts to address insect resistance stewardship challenges. *Pestic. Biochem. Physiol.* 106, 76–78.
- Vontas, J., Katsavou, E., Mavridis, K., 2020. Cytochrome P450-based metabolic insecticide resistance in *Anopheles* and *Aedes* mosquito vectors: muddy the waters. *Pestic. Biochem. Physiol.* 170, 104666.
- Wang, R., Zhu, Y., Deng, L., Zhang, H., Wang, Q., Yin, M., Song, P., Elzaki, M.E.A., Han, Z., Wu, M., 2017. Imidacloprid is hydroxylated by *Laodelphax striatellus* CYP6AY3v2. *Insect Mol. Biol.* 26, 543–551.
- Wang, X.G., Chen, Y.Q., Gong, C.W., Yao, X.G., Jiang, C.X., Yang, Q.F., 2018. Molecular identification of four novel cytochrome P450 genes related to the development of resistance of *Spodoptera exigua* (Lepidoptera: Noctuidae) to chlorantraniliprole. *Pest Manag. Sci.* 74, 1938–1952.
- Wang, C.N., Qin, Y.F., Li, Y.L., Wu, R.L., Zhu, D.Q., Zhou, F., Xu, F.L., 2021. Variations of root-associated bacterial cooccurrence relationships in paddy soils under chlorantraniliprole (CAP) stress. *Sci. Total Environ.* 779, 146247.
- Wu, M., Li, G.L., Chen, X.F., Liu, J., Liu, M., Jiang, C.Y., Li, Z.P., 2018a. Rational dose of insecticide chlorantraniliprole displays a transient impact on the microbial metabolic functions and bacterial community in a silty-loam paddy soil. *Sci. Total Environ.* 616–617, 236–244.
- Wu, Y., Yang, J., Duan, C.L., Chu, L.X., Chen, S.H., Qiao, S., Li, X.M., Deng, H.H., 2018b. Simultaneous determination of antiretroviral drugs in human hair with liquid chromatography-electrospray ionization-tandem mass spectrometry. *J. Chromatogr. B* 1083, 209–221.
- Xu, L., Zhao, J., Sun, Y., Xu, D.J., Xu, G.C., Xu, X.L., Zhang, Y.L., Huang, S.J., Han, Z.J., Gu, Z.Y., 2019. Constitutive overexpression of cytochrome P450 monooxygenase genes contributes to chlorantraniliprole resistance in *Chilo suppressalis* (Walker). *Pest Manag. Sci.* 75, 718–725.
- Xu, L., Zhao, J., Xu, D.J., Xu, G.C., Gu, Z.Y., Xiao, Z., Dewer, Y., Zhang, Y.N., 2022. Application of transcriptomic analysis to unveil the toxicity mechanisms of fall armyworm response after exposure to sublethal chlorantraniliprole. *Ecotoxicol. Environ. Saf.* 230, 113145.
- Yang, L.P., Wang, S.Y., Wang, R.F., Zheng, Q., Ma, Q.L., Huang, S.Q., Chen, J.J., Zhang, Z.X., 2021. Floating chitosan-alginate microspheres loaded with chlorantraniliprole effectively control *Chilo suppressalis* (Walker) and *Sesamia inferens* (Walker) in rice fields. *Sci. Total Environ.* 783, 147088.
- Yin, H.M., Huang, Y., Yan, G.W., Huang, Q., Wang, Y., Liu, H.M., Huang, Z.Q., Hong, Y.H., 2023. Effects of chlorantraniliprole-based pesticide on transcriptional response and gut microbiota of the crucian carp, *Carassius carassius*. *Ecotoxicol. Environ. Saf.* 263, 115292.
- Zhang, Y.X., Yang, Y.X., Sun, H.H., Liu, Z.W., 2016. Metabolic imidacloprid resistance in the brown planthopper, *Nilaparvata lugens*, relies on multiple P450 enzymes. *Insect Biochem. Mol. Biol.* 79, 50–56.
- Zhu, Q.Y., Li, F.C., Shu, Q.L., Feng, P., Wang, Y.F., Dai, M.L., Mao, T.T., Sun, H.N., Wei, J., Li, B., 2023. Disruption of peritrophic matrix chitin metabolism and gut immune by chlorantraniliprole results in pathogenic bacterial infection in *Bombyx mori*. *Pestic. Biochem. Physiol.* 193, 105430.
- Zimmer, C.T., Garrood, W.T., Singh, K.S., Randall, E., Lueke, B., Gutbrod, O., Matthiesen, S., Kohler, M., Nauen, R., Davies, T.G.E., Bass, C., 2018. Neofunctionalization of duplicated P450 genes drives the evolution of insecticide resistance in the brown planthopper. *Curr. Biol.* 28, 268–274.
- Zong, M., Yu, C., Li, J.Q., Sun, D., Wang, J.Y., Mo, Z.Y., Qin, C.W., Yang, D.S., Zhang, Z.Y., Zeng, Q.H., Li, C.Y., Ma, K.S., Wan, H., Li, J.H., He, S., 2023. Redox and near-infrared light-responsive nanoplateform for enhanced pesticide delivery and pest control in rice: construction, efficacy, and potential mechanisms. *ACS Appl. Mater. Interfaces* 15, 41351–41361.